

1  **$J/\psi$  production within a jet in p+p collisions at  $\sqrt{s} = 500$**   
2 **GeV by STAR**

---

3 **Qian Yang (for the STAR Collaboration)<sup>a,\*</sup>**

4 <sup>a</sup>*Shandong University,*

5 *No.27 Binhai Road, Qingdao, China*

6 *E-mail: [yangqian2020@sdu.edu.cn](mailto:yangqian2020@sdu.edu.cn)*

The suppression of  $J/\psi$  production caused by the color-screening effect in heavy-ion collisions is considered as an evidence of the creation of quark-gluon plasma. However, the production of  $J/\psi$  in hadronic collisions remains not fully understood. Further studies are needed to provide a good understanding of its production mechanism in p+p collisions for interpreting the observed suppression in heavy-ion collisions. Recently, the  $J/\psi$  production in jets was proposed as a useful observable to help explore the  $J/\psi$  production mechanism and to differentiate various  $J/\psi$  production models.

7 We report the measurement of the fraction of charged jet transverse momentum carried by the  $J/\psi$  meson,  $z(J/\psi) \equiv p_T^{J/\psi}/p_T^{\text{jet}}$ , at mid-pseudorapidity ( $|\eta| < 0.6$ ) with kinematic cuts of  $p_T^{\text{jet}} > 10$  GeV/c and  $p_T^{J/\psi} > 5$  GeV/c in p+p collisions at  $\sqrt{s} = 500$  GeV by the STAR experiment. The comparison to model calculations and similar measurements carried out at the LHC are presented, and its physics implications are discussed.

*HardProbes2020*

*1-6 June 2020*

*Austin, Texas*

---

\*Speaker

## 1. Introduction

The  $J/\psi$  meson is a bound state of charm and anti-charm quarks ( $c\bar{c}$ ) and was discovered several decades ago.  $J/\psi$  is a multiscale system. Production of charm and anti-charm pairs can be described by perturbative quantum chromodynamics (QCD), but the evolution of charm and anti-charm quark pair to a  $J/\psi$  is a nonperturbative process which can only rely on phenomenological model description. Thus, studying its production provides valuable knowledge for the understanding of all regimes of QCD. However, the  $J/\psi$  production mechanism results in a rich phenomenology that is yet to be fully understood [1].

The most successful approach of describing  $J/\psi$  production in hadronic collisions is the nonrelativistic QCD (NRQCD) factorization formalism [2]. In NRQCD models, the evolution of  $c\bar{c}$  pairs of different quantum states to  $J/\psi$  is characterized by a set of universal NRQCD long-distance matrix elements (LDMEs). Differential  $J/\psi$  production cross section measurements in p+p system from RHIC to the LHC energies can be well described by the NRQCD approach [2]. However, the LDMEs extracted by different groups show significant difference [3]. Furthermore, experimental measurements showed minimal  $J/\psi$  polarization which contradicts to the large degree of transverse polarization from the NRQCD predictions [4]. These discrepancies indicate that further studies are needed to gain a better understanding of the  $J/\psi$  production.

Recently, Ref [5] showed that  $J/\psi$  production within a jet provides a strong discriminative power for different models, and thus can be used to study the  $J/\psi$  production mechanism. At the LHC, LHCb collaboration and CMS collaboration reported their measurements of  $J/\psi$  production within a jet [6, 7]. The discrepancies between measurements and the NRQCD predictions are shown in Ref [8]. Measuring the  $J/\psi$  production within a jet at a very different collision energy will provide further insight to the  $J/\psi$  production mechanism.

## 2. Experiment and Analysis

The data sample used in this analysis was collected from p+p collisions at  $\sqrt{s} = 500$  GeV in 2011 by the STAR experiment. The integrated luminosity of the data set is  $22.1 \text{ pb}^{-1}$  sampled by the Barrel Electromagnetic Calorimeter (BEMC) trigger which requires a BEMC tower with an energy deposition larger than 4.3 GeV. The  $J/\psi \rightarrow e^+e^-$  decay channel is used for  $J/\psi$  reconstruction. Electron and positron candidates are reconstructed and identified using information from the TPC and BEMC detectors. The details of  $e^\pm$  candidates selection and the  $J/\psi$  reconstruction can be found in Ref [9].

With a  $J/\psi$  candidate in an event, jet reconstruction is performed on this event by clustering the  $J/\psi$  candidate with charged particles. The  $J/\psi$  candidates, rather than their decayed  $e^\pm$ , are used in the clustering to prevent  $e^\pm$  from the same  $J/\psi$  decay being clustered into separate jets. The jet reconstruction using the anti- $k_T$  clustering algorithm as implemented in the FASTJET package [10] and the jet cone size is set to  $R = 0.2, 0.4$  and  $0.6$ . Events passing kinematic cuts for reconstructed jets ( $p_T > 10 \text{ GeV}/c$ ,  $|\eta^{\text{jet}}| < 1-R$ ) and  $J/\psi$  candidates ( $p_T^{J/\psi} > 5 \text{ GeV}/c$  and  $|\eta^{J/\psi}| < 1$ ) are kept for further analysis, where  $p_T$  and  $\eta$  denote transverse momentum and pseudo-rapidity, respectively.

The yield of  $J/\psi$  in each  $z(J/\psi) \equiv p_T^{J/\psi} / p_T^{\text{jet}}$  bin is extracted from corresponding  $e^+e^-$  invariant mass distribution with detector efficiency and acceptance corrected for. Figure 1 shows an example

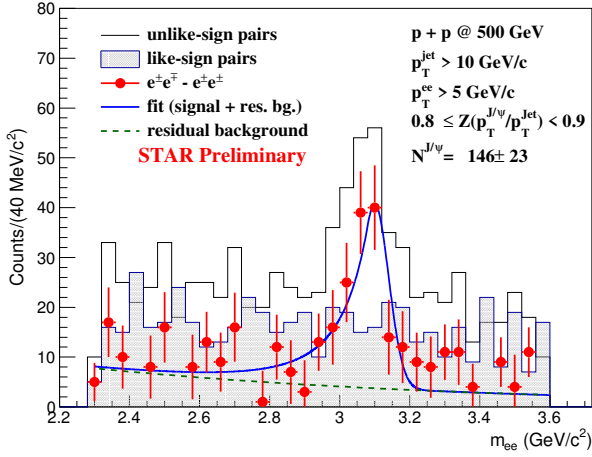


**Figure 1:** Invariant mass distributions of  $e^+e^-$  pairs before and after the like-sign background (gray filled histogram) subtraction as shown in black histogram and red solid circles, respectively. The blue curve is a fit to the mass spectrum. The green-dashed line indicates the residual background and a Crystal-Ball function is used to describe the  $J/\psi$  signal. The error bars depict the statistical uncertainties.

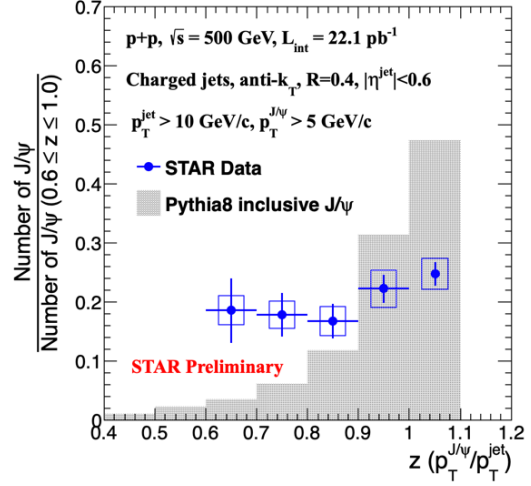


**Figure 2:** Self-normalized  $z$  distributions for inclusive  $J/\psi$  mesons produced within a jet compared to prediction from PYTHIA 8 (gray filled histogram). The vertical blue lines represent statistical uncertainties and the blue boxes represent systematic uncertainties. The data point for isolated  $J/\psi$  ( $z = 1$ ) is placed at 1.05 for clarity.

48 of such  $e^+e^-$  invariant mass distributions for  $0.8 \leq z < 0.9$ . The detector effects on reconstructed  
49 jet  $p_T$  and  $z(J/\psi)$  are accounted for via two-dimensional unfolding [11].

### 50 3. Physics Results

51 Figure 2 shows self-normalized  $z(J/\psi)$  distribution for inclusive  $J/\psi$  mesons produced within  
52 a charged jet for  $p_T^{\text{jet}} > 10$  GeV/c and  $p_T^{J/\psi} > 5$  GeV/c. The data point for isolated  $J/\psi$  ( $z = 1$ )  
53 is placed at 1.05 for clarity. With current uncertainties, there is no significant  $z(J/\psi)$  dependence for  
54  $z < 1$  range. Figure 3 shows the jet cone size ( $R$ ) dependence in the same kinematic cuts for jets  
55 and  $J/\psi$  as in Fig. 2. A hint of  $R$  dependence is observed, but more statistics is needed to draw firm  
56 conclusions. The analysis using a large data sample with an integrated luminosity of  $336.4 \text{ pb}^{-1}$   
57 from 2017 is ongoing, which will significantly improve the precision of the measurement.

58 Figure 2 also shows comparison between the measurement and the leading-order (LO) NRQCD-  
59 based PYTHIA 8 prediction [12]. The measured self-normalized  $z$  distribution shows a different  
60 trend than the prediction, i.e.  $J/\psi$  production within a jet is less isolated in data than that predicted by  
61 PYTHIA 8. Experimental measurements at LHC energies [6, 7] also show a less isolated production  
62 scenario for  $J/\psi$  produced within a jet than PYTHIA predictions, despite of very different collision  
63 energy, rapidity range as well as jet definition compared to this analysis. It is also informative to  
64 study the fraction of  $J/\psi$  produced within a jet, as shown in Fig. 4. The y-axis is the ratio of number  
65 of  $J/\psi$  within a jet for  $p_T^{J/\psi} > 5$  GeV/c and  $p_T^{\text{jet}} > 10$  GeV/c to the total number of  $J/\psi$  with  $p_T > 5$   
66 GeV/c. The  $J/\psi$  cross section with  $p_T^{J/\psi} > 5$  GeV/c is measured in Ref [9]. The results show that

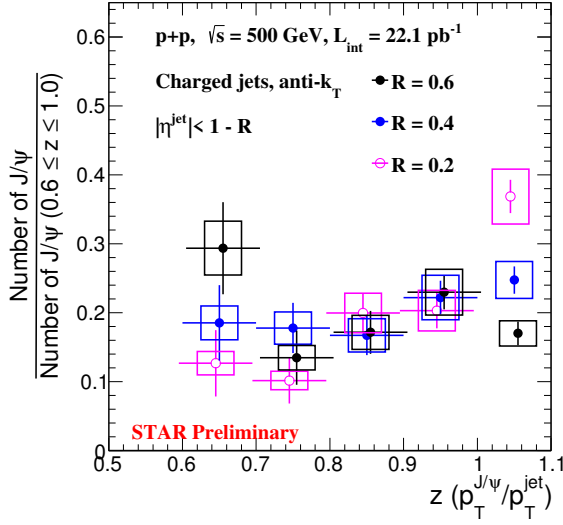


**Figure 3:** Self-normalized  $z$  distributions for inclusive  $J/\psi$  mesons produced within a jet for different jet cone size of 0.2, 0.4 and 0.6. The error bars represent statistical uncertainties and the blue boxes represent systematic uncertainties.

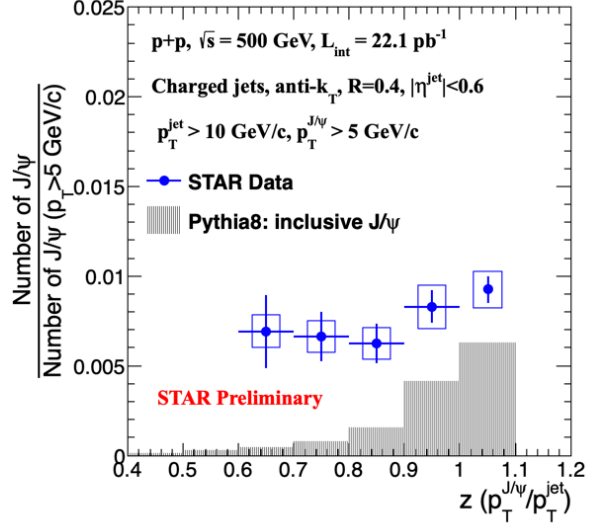


**Figure 4:** The normalized  $z$  distributions for inclusive  $J/\psi$  mesons produced within a jet compared to prediction from PYTHIA 8. The data is normalized by the  $J/\psi$  cross-section with  $p_T^{J/\psi} > 5$  GeV/c at the same collision energy [9].

67 the probability of producing a  $J/\psi$  above 5 GeV/c in a charged jet above 10 GeV/c is systematically  
68 higher in data than in PYTHIA 8.

#### 69 4. Summary

70 The fraction of charged jet transverse momentum carried by the  $J/\psi$  meson at mid-pseudorapidity  
71 ( $|\eta| < 0.6$ ) with kinematic cuts of  $p_T^{\text{jet}} > 10$  GeV/c and  $p_T^{J/\psi} > 5$  GeV/c in  $p+p$  collisions at  $\sqrt{s} =$   
72 500 GeV is measured. It is the first measurement of  $J/\psi$  production within a jet at RHIC energy.  
73 The observed  $z(J/\psi)$  distribution does not show a significant  $z(J/\psi)$  dependence for  $z < 1$  within  
74 current uncertainties. A hint of jet cone size dependence is observed, but more statistics is needed  
75 to draw firm conclusions. Compared to PYTHIA 8 predictions with the same kinematic cuts,  $J/\psi$   
76 production within a jet is less isolated and more  $J/\psi$  are produced in jets in the measured kinematic  
77 range in data.

#### 78 Acknowledgements

79 The work is partly supported by the Program of Young Scholars Future Plan in Shandong  
80 University and the Shandong Provincial Natural Science Foundation, China (No. ZR2019MA005).

#### 81 References

82 [1] N. Brambilla, S. Eidelman et al, Eur. Phys. J.C. 71, 1534 (2011).

- 83 [2] Yan-Qing Ma and Raju Venugopalan, Phys. Rev. Lett. 113, 192301 (2014).
- 84 [3] Jean-Philippe Lansberg, arXiv:1903.09185.
- 85 [4] A. Andronic et al., Eur. Phys. J.C. 76,107 (2016).
- 86 [5] Zhong-Bo Kang, Jian-Wei Qiu et al., Phys. Rev. Lett. 119, 032001 (2017).
- 87 [6] R. Aaij et al. (LHCb Collaboration), Phys. Rev. Lett. 118, 192001 (2017).
- 88 [7] A.M. Sirunyan et al. (CMS Collaboration), Phys. Lett. B 804, 1354091 (2020).
- 89 [8] Reggie Bain, Yiannis Makris, and Thomas Mechen, Phys. Rev. Lett. 119, 032002 (2017).
- 90 [9] J. Adam et al. (STAR Collaboration), Phys. Rev. D 100, 052009 (2019).
- 91 [10] M. Cacciari, G. P. Salam, and G. Soyez, Eur. Phys. J. C 72, 1896 (2012).
- 92 [11] G. D'Agostini, Nucl. Instrum. Methods Phys. Res., Sect. A 362, 487 (1995).
- 93 [12] T. Sjostrand, S. Mrenna, and P. Skands, Comput. Phys. Commun. 178, 852 (2008).